SSRG International Journal of Electrical and Electronics Engineering
ISSN: 2348-8379/ https://doi.org/10.14445/23488379/IJEEE-V10I4P117

Volume 10 Issue 4, 169-174, April 2023

Original Article

Development of an Algorithm that Allows Improving Disparity Maps in Environments Contaminated with Suspended Particles

John Kern[1], Javier Silva[2], Claudio Urrea[3]

[1,2,3] *Electrical Engineering Department, University of Santiago de Chile, Santiago, Chile*

[1]*Corresponding Author : john.kern@usach.cl*

Received: 04 March 2023 Revised: 31 March 2023 Accepted: 18 April 2023 Published: 30 April 2023

Abstract *- The estimation of the depth of a scene has become a research niche due to the large number of applications that exist today. In a stereo vision system, disparity maps make it possible to obtain the depth of a scene from two rectified images. Stereo vision systems are sensitive to illumination, reflections, lens distortion, noise, camera alignment, etc.; therefore, in this work, we present an algorithm that allows us to improve the disparity map when the environment presents particles in suspension using stereo vision through infrared cameras. For this purpose, filters, matching, and dehazing algorithms are implemented.*

Keywords *- Disparity map, Stereo Vision, Semi-Global Block Matching, Dehazing algorithm, Weighted Least Squares filter.*

1. Introduction

Since the development of cameras, it has been proposed to provide machines with vision so that they can perform operations similar to those a human would do. Human beings have the ability to use, analyze and understand the three-dimensional objects that surround them with great ease. This is due to the fact that they have two eyes (known as binocular vision), which gives the brain the ability to extract information about the depth of the scenes [1]. Currently, many sensors and techniques focus on 3D vision, such as using Time of Flight (ToF) sensors, Microsoft Kinects sensors, structured light projection, Laser Imaging Detection and Ranging (LIDAR) sensors, etc. The newest methods for 3D vision point to the use of monocular vision and artificial intelligence (AI); some of them can be found in [2], [3]. Despite the great advances and rapid growth in the field of AI, without a doubt, the most widely used technique in volumetric reconstruction has been stereo vision [4]. Stereo vision (SV) is inspired by the human vision system, which makes it possible to obtain the depth of a scene by analyzing two images of the same scene but taken from two different points. A previous step to obtain the point cloud of the scene under study is to obtain a disparity map. A disparity map represents the horizontal displacement of the pixels between the left and right image [5].

While ToF and Kinect devices are inexpensive and have attracted the attention of researchers, these sensors are subject to errors such as noise and ambiguity and are also subject to non-systematic errors such as motion dispersion and motion blur [5], [6]. Also, ToF devices perform satisfactorily within a range but are highly sensitive for use in outdoor environments, especially in brightly lit areas. For these reasons, SV systems are more reliable and robust for producing disparity maps for both indoor and outdoor environments [5]. However, the acquired images may contain too much noise in poorly controlled environments and produce poor image processing results. A solution to this problem is improving the hardware, which makes the solution very expensive [7]. Although algorithms have improved their accuracy and performance considerably, disparity prediction is still prone to erroneous or inaccurate estimates, especially in ambiguous regions [8]. In addition to the above, it can be said that a large part of the algorithms for obtaining disparity maps are applied to synthetic images or controlled environments. With the abovementioned foundations, the contribution of the paper highlights the obtaining of the disparity map in a dust-cloudy environment and the use of a stereoscopic system of infrared (IR) cameras to estimate the shape of the rocks that will later be applied in mining comminution processes.

2. Related Works

Algorithms for obtaining disparity maps show a constant development and improvement of their techniques in recent years, including seeking to achieve real-time applications such as autonomous driving, 3D games, and autonomous robotic navigation [5]. Next, new algorithms developed during the last year are discussed, which shows that it is an active research topic.

In [10], the authors define that the algorithms to obtain disparity maps have four parts: matching cost calculation, cost aggregation, disparity calculation, and disparity refinement. Some of the recent algorithms propose improvements in some of the mentioned steps to optimize the accuracy of disparity maps.

The most recent algorithms point to the use of AI due to the satisfactory results it has had in the field of computer vision. Such is the case of [8], who make use of the disparity map produced by traditional algorithms, to create a confidence map on the raw disparities and then use a self-supervised Deep Neural Network (DNN), which predicts a map with more precise disparity. In [11], an algorithm capable of calculating a semi-dense disparity map is presented, which is then completed with the monocular signals from each camera. This method allows for handling both positive and negative disparities, which has applications in augmented reality or virtual reality. In [12], you can see an architecture using convolutional neural networks (CNN). In the first instance, they use a 2-D CNN to extract features from the left and right image, then form a 4-D feature map that subsequently enters a 3-D CNN to produce the result without any post-processing of the disparity map.

A post-processing technique for improving noisy disparity maps can be seen in [13]. The technique is based on discarding pixels assigned with huge disparities, then filtering the map and evaluating the colors of the original images using the support weighted window method with a modification.

In [14], they propose to eliminate the expensive 3D convolution operation, and for this purpose, they introduce two modules to improve the cost aggregation process. The results of [14] are produced in just 62 milliseconds with excellent accuracy.

On the other hand, some techniques don't use AI to obtain disparity maps, such as the case of [15,17,18].

In [15], propose a method to improve the resolution of disparity maps based on dual dynamic programming. The method consists of obtaining two disparity maps (using both images as reference), applying a vertical smoothing technique, and then integrating both disparity maps. The work proposed in [17] uses the four steps described by [10]; they use Census transform for cost calculation, segment tree for cost aggregation, winner-takes-all (WTA) strategy for disparity calculation, and weighted median filter for disparity refinement. On the other hand, the authors of [18]propose an improvement to the AD-Census algorithm, which reduces the noise that the traditional Census transform is affected, improving the contours of the objects within the disparity map.

Regarding stereo image matching in cloudy environments with low visibility, three types of solutions can be found [19]:

1. Those who consider the fog as noise and discard it to carry out the stereo-matching process later (either through a dehazing algorithm or using specific hardware)
2. Those methods seek to create algorithms robust to noise.
3. Those methods use fog to aid stereo matching.

As part of the first solution, some recent works can be found, such as [20] and [21]. In [20], they propose GCANet, a network which makes use of dilated convolution to add context information without sacrificing resolution. In [21], the U-Net [20] architecture is used to propose a dense feature fusion module, together with a Strengthen-Operate-Subtract (SOS) [24] reinforcement strategy, to achieve image restoration.

Regarding the second solutions can find [25] and [26]. In [25], disparity maps are produced using confidence measures for general outdoor environments. On the other hand, [26] proposes an algorithm that allows deep stereo methods to adapt to the environment in an unsupervised manner. Finally, the third type solution is [19], which proposes collecting information about the fog volume and then generating the image restoration by rendering.

A review of various methods to improve images in environments affected by adverse conditions can be found in [27] and [28].

3. Proposed Work

The proposed work consists of capturing photographs in dust-cloudy environments and obtaining the disparity map using low-cost elements. In this work, we have chosen not to use AI because there are no rock databases for training AI models; in addition, the rocks to be treated are amorphous solids that do not follow any pattern, so machine vision algorithms are used. The technique employed consists of the first type of algorithms, i.e., removing the cloud from each image using the Fast Dark Channel Prior algorithm (proposed in [29]), then applying filters and finally applying the Semi-Global Block Matching (SGBM) algorithm, followed by the weighted least squares (WLS) filter. The algorithm used can be visualized in Figure 1.

The experiment developed consists of a closed system of 120x50x30 centimeters (cm), with two security cameras at the top with night vision of the YI IoT brand, which was intervened always to operate the infrared camera. The resolution of the images captured by the cameras is 360x640 pixels (px). On the side, there is a tube that allows the entry of particulate material and airflow. When the airflow encounters the particulate material, it produces a dust cloud that reduces the visibility of the cameras. A graphic representation of the model under study is shown in Figure 2.

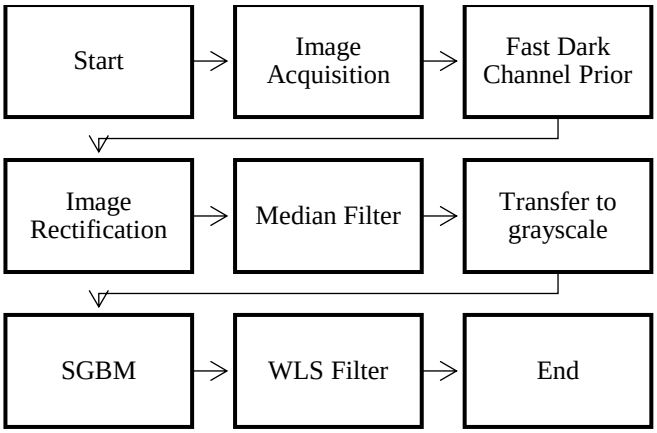

Fig. 1 Flowchart for obtaining the disparity map

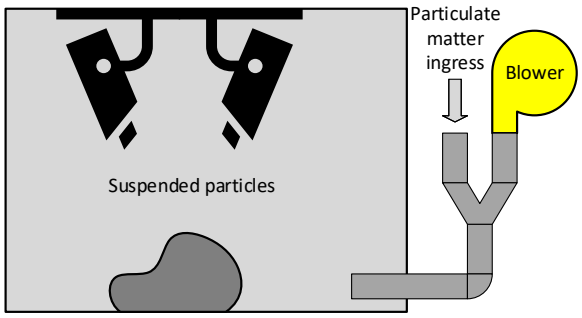

Fig. 2 Proposed experiment

The images without suspended particles and without rectification can be seen in Figure 3. Once the blower is turned on, the dust cloud is lifted, and after 10 seconds, the photograph is captured and shown in Figure 4.

It is possible to obtain an initial disparity map (after rectification) for both cases of Figure 3 and Figure 4. Figure 5 and Figure 6 show the result of applying the SGBM algorithm, with a block size of 11x11 pixels, considering a maximum disparity of 150 px. A poor and discontinuous disparity map can be appreciated. The results of the proposed algorithm will be shown in the next section.

Fig. 5 Disparity map obtained by the SGBM algorithm for an environment without suspended particles

Fig. 6 Disparity map obtained by the SGBM algorithm for an environment with suspended particles

Fig. 3 Input images without suspended particles

Fig. 4 Input images with suspended particles

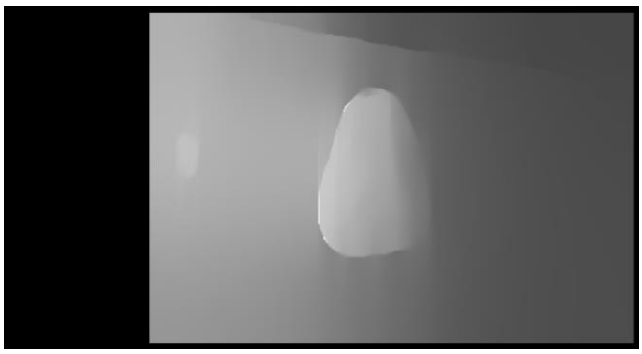

Fig. 7 Disparity map obtained with the proposed algorithm

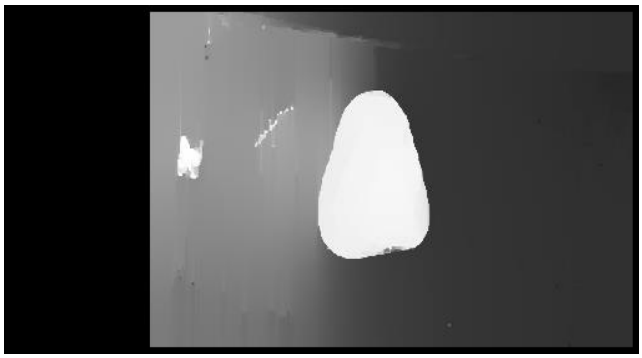

Fig. 8 Disparity map GT

4. Results and Discussion

Figure 7 shows the result of the proposed algorithm when the environment is subjected to a cloud of dust. At first glance, you can see a great improvement in the disparity map compared to Figure 5 and Figure 6.

In search to obtain a quantitative evaluation of the disparity map obtained, the algorithm proposed in Figure 1 has been implemented to the images without suspended particles in Figure 3, obtaining; as a result, the disparity map of Figure 8, which will be considered as ground truth (GT) of the algorithm. Based on the GT, the comparison metrics can be seen in Table I.

It is possible to appreciate that all the metrics of the proposed algorithm far exceed the SGBM algorithm. On the other hand, Figures 9 and 10 present the information in Table I graphically to visualize the large difference between the metrics.

Table 1. Comparison metrics for the proposed algorithm

Metrics	Proposed Algorithm	SGBM
RMS Error	0.1136	0.22
BMP	0.067	0.659
Mean Absolute Error	5.58	52.32
Mean square error	17.027	165.34
PSNR	16.588	10.45
SSIM	0.909	0.305

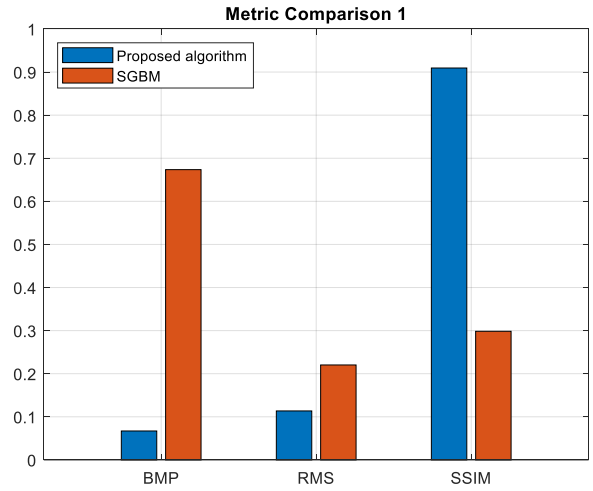

Fig. 9 Graphical comparison of BMP, RMS, and SSIM metrics

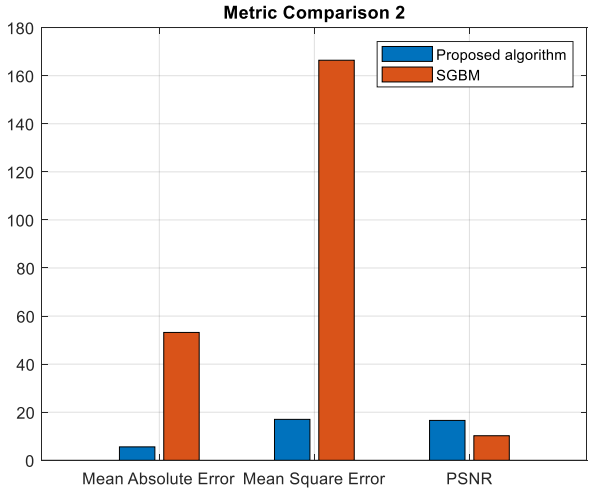

Fig. 10 Graphical comparison of MAE, MSE and PSNR metrics

An important parameter when running the SGBM algorithm is the size of the matching window. This parameter is vital to achieve good results. This is why a test of the dynamics of the error metrics as a function of the size of the matching window has been developed. Figure 11 shows the evolution of the metrics Root Mean Square (RMS) error, Bad Matching Pixels (BMP), and Structural Similarity Index Measure (SSIM). From the graph, it can be seen that there is an optimum point for the SSIM, while BMP increases as the window increases.

On the other hand, the RMS error suffers unpredictable variations. The present work has focused on optimizing SSIM since many of the metrics presented in Table 1 are easy to interpret but are not closely related to the visual quality perceived by humans [16]. In addition, SSIM does not require a threshold like BMP, which transforms BMP into a subjective metric. According to Figure 11, the maximum SSIM is achieved with an 11x11 pixel window, which was applied to achieve the result of Figure 7.

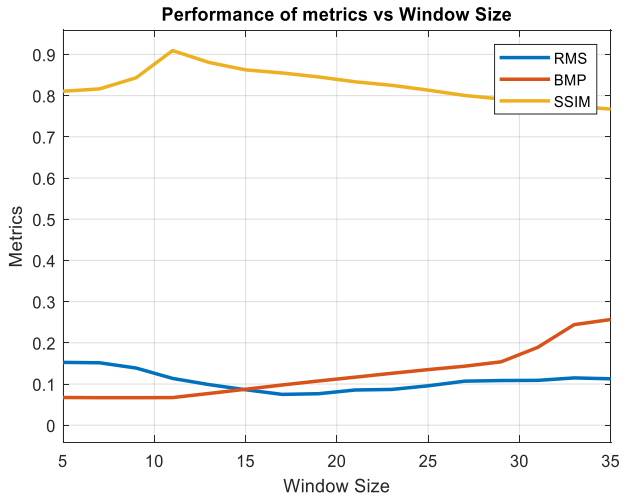

Fig. 11 Graph of the variation of the metrics as a function of the block size of the SGBM algorithm

5. Conclusion

From the development of the work, it is possible to conclude that:

- It is possible to improve the disparity map in an environment with suspended particles through filtering and dehazing techniques.
- A dehazing algorithm can be applied to remove the effect of dust from photos.
- The dehazing algorithm depends on the dispersion coefficient of the atmosphere; the higher the value of the coefficient, the greater the haze removal effect, but the darker the resulting image, so other image processing algorithms must be applied.
- Despite having identical cameras from the same supplier, they do not capture images with the same quality, this is because the cameras used are low-cost and do not have some degree of protection, so it is possible that during the execution of the experiments, dust may have infiltrated inside the cameras.

Funding Statement

This work has been supported by Agencia Nacional de Investigación y Desarrollo ANID, Chile, through the IDeA I+D ID21I10087 project and by Vicerrectoría de Investigación, Desarrollo e Innovación of the University of Santiago of Chile, Chile.

References

[1] E. R. Davies, *Computer and Machine Vision: Theory, Algorithms, Practicalities*, 4th edition. Waltham, Mass: Elsevier, 2012. [Google Scholar] [Publisher Link]

[2] George Fahim, Khalid Amin, and Sameh Zarif, "Single-View 3D Reconstruction: A Survey of Deep Learning Methods," *Computers & Graphics*, vol. 94, pp. 164-190, 2021. [CrossRef] [Google Scholar] [Publisher Link]

[3] Xian-Feng Han, Hamid Laga, and Mohammed Bennamoun, "Image-Based 3D Object Reconstruction: State-of-the-Art and Trends in the Deep Learning Era," *IEEE Transactions on Pattern Analysis and Machine Intelligence*, vol. 43, no. 5, pp. 1578-1604, 2021. [CrossRef] [Google Scholar] [Publisher Link]

[4] Andrew O'Riordan et al., "Stereo Vision Sensing: Review of Existing Systems," *2018 12th International Conference on Sensing Technology*, pp. 178-184, 2018. [CrossRef] [Google Scholar] [Publisher Link]

[5] Rostam Affendi Hamzah, and Haidi Ibrahim, "Literature Survey on Stereo Vision Disparity Map Algorithms," *Journal of Sensors*, vol. 2016, p. 8742920, 2015. [CrossRef] [Google Scholar] [Publisher Link]

[6] Pietro Zanuttigh et al., "Operating Principles of Time-of-Flight Depth Cameras," *Time-of-Flight and Structured Light Depth Cameras: Technology and Applications*, P. Zanuttigh, G. Marin, C. Dal Mutto, F. Dominio, L. Minto, y G. M. Cortelazzo, Eds., Cham: Springer International Publishing, pp. 81-113, 2016. [CrossRef] [Google Scholar] [Publisher Link]

[7] Phuong Ngoc Binh Do, and Quoc Chi Nguyen, "A Review of Stereo-Photogrammetry Method for 3-D Reconstruction in Computer Vision," *2019 19th International Symposium on Communications and Information Technologies (ISCIT)*, pp. 138-143, 2019. [CrossRef] [Google Scholar] [Publisher Link]

[8] Xiule Fan, Soo Jeon, and Baris Fidan, "Occlusion-Aware Self-Supervised Stereo Matching with Confidence Guided Raw Disparity Fusion," *2022 19th Conference on Robots and Vision (CRV)*, pp. 132-139, 2022. [CrossRef] [Google Scholar] [Publisher Link]

[9] Nilesh Dubey, and Hardik Modi, "A State of Art Comparison of Robust Digital Watermarking Approaches for Multimedia Content (Image and Video) Against Multimedia Device Attacks," *International Journal of Engineering Trends and Technology*, vol. 70, no. 8, pp. 132-139, 2022. [CrossRef] [Google Scholar] [Publisher Link]

[10] D. Scharstein, R. Szeliski, and R. Zabih, "A Taxonomy and Evaluation of Dense Two-Frame Stereo Correspondence Algorithms," *Proceedings IEEE Workshop on Stereo and Multi-Baseline Vision (SMBV 2001)*, pp. 131-140, 2001. [CrossRef] [Google Scholar] [Publisher Link]

[11] Jiazhi Liu, and Feng Liu, "A Novel Stereo Matching Pipeline with Robustness and Unfixed Disparity Search Range," *2022 IEEE International Conference on Multimedia and Expo (ICME)*, pp. 1-6, 2022. [CrossRef] [Google Scholar] [Publisher Link]

[12] Wen-Nung Lie, Hung-Ta Chiu, and Jui-Chiu Chiang, "Disparity Map Estimation From Stereo Image Pair Using Deep Convolutional Network," *2020 International Computer Symposium (ICS)*, pp. 365-369, 2020. [CrossRef] [Google Scholar] [Publisher Link]

[13] Gabriel da Silva Vieira et al., "Disparity Map Adjustment: a Post-Processing Technique," *2018 IEEE Symposium on Computers and Communications*, pp. 00580-00585, 2018. [CrossRef] [Google Scholar] [Publisher Link]

[14] Haofei Xu, and Juyong Zhang, "AANet: Adaptive Aggregation Network for Efficient Stereo Matching," *2020 IEEE/CVF Conference on Computer Vision and Pattern Recognition (CVPR)*, pp. 1956-1965, 2020. [CrossRef] [Google Scholar] [Publisher Link]

[15] Monika Gupta, Sapna Malik, "Dual Dynamic Programming with quantization for disparity map," SSRG International Journal of Computer Science and Engineering , vol. 4, no. 3, pp. 5-9, 2017. [CrossRef] [Google Scholar] [Publisher Link]

[16] Ivan Cabezas, Victor Padilla, and Maria Trujillo, *A Measure for Accuracy Disparity Maps Evaluation*, vol. 7042, p. 231, 2011. [CrossRef] [Google Scholar] [Publisher Link]

[17] Muhammad Nazmi Zainal Azali et al., "Stereo Matching Algorithm Using Census Transform and Segment Tree for Depth Estimation," *TELKOMNIKA Telecommunication Computing Electronics and Control*, vol. 21, no. 1, p. 150, 2023. [CrossRef] [Google Scholar] [Publisher Link]

[18] Yina Wang et al., "Improvement of AD-Census Algorithm Based on Stereo Vision," *Sensors*, vol. 22, no. 18, 2022. [CrossRef] [Google Scholar] [Publisher Link]

[19] Chengtang Yao, and Lidong Yu, "FoggyStereo: Stereo Matching with Fog Volume Representation," *2022 IEEE/CVF Conference on Computer Vision and Pattern Recognition (CVPR)*, pp. 13033-13042, 2022. [CrossRef] [Google Scholar] [Publisher Link]

[20] Dongdong Chen et al., "Gated Context Aggregation Network for Image Dehazing and Deraining," *2019 IEEE Winter Conference on Applications of Computer Vision (WACV)*, pp. 1375-1383, 2019. [CrossRef] [Google Scholar] [Publisher Link]

[21] Hang Dong et al., "Multi-Scale Boosted Dehazing Network With Dense Feature Fusion," *2020 IEEE/CVF Conference on Computer Vision and Pattern Recognition (CVPR)*, pp. 2154-2164, 2020. [CrossRef] [Google Scholar] [Publisher Link]

[22] Venkat P. Patil, and C. Ram Singla, "Performance Enhancement of Image Stitching Process Under Bound Energy aided feature matching and Varying Illumination Environments," *SSRG International Journal of Electronics and Communication Engineering*, vol. 6, no. 9, pp. 1-6, 2019. [CrossRef] [Publisher Link]

[23] Olaf Ronneberger, Philipp Fischer, and Thomas Brox, "U-Net: Convolutional Networks for Biomedical Image Segmentation," *Medical Image Computing and Computer-Assisted Intervention – MICCAI 2015*, N. Navab, J. Hornegger, W. M. Wells, y A. F. Frangi, Eds., Cham: Springer International Publishing, pp. 234-241, 2015. [CrossRef] [Google Scholar] [Publisher Link]

[24] Y Yaniv Romano, and Michael Elad, "SOS Boosting of Image Denoising Algorithms," *CoRR*, 2015. [CrossRef] [Google Scholar] [Publisher Link]

[25] Min-Gyu Park, and Kuk-Jin Yoon, "Leveraging Stereo Matching with Learning-Based Confidence Measures," *2015 IEEE Conference on Computer Vision and Pattern Recognition (CVPR)*, pp. 101-109, 2015. [CrossRef] [Google Scholar] [Publisher Link]

[26] Alessio Tonioni et al., "Learning to Adapt for Stereo," *2019 IEEE/CVF Conference on Computer Vision and Pattern Recognition (CVPR)*, pp. 9653-9662, 2019. [CrossRef] [Google Scholar] [Publisher Link]

[27] R. Suganya, and D. R. Kanagavalli, "On the Review of Dehazing Methods for Bad Weather Images," *International Journal of Engineering Trends and Technology*, 2020. [Publisher Link]

[28] Shilong Liu et al., "Dark Channel Prior Based Image De-Hazing: A Review," *2015 5th International Conference on Information Science and Technology (ICIST)*, pp. 345-350, 2015. [CrossRef] [Google Scholar] [Publisher Link]

[29] Wencheng Wang et al., "A Fast Single-Image Dehazing Method Based on a Physical Model and Gray Projection," *IEEE Access*, vol. 6, pp. 5641-5653, 2018. [CrossRef] [Google Scholar] [Publisher Link]